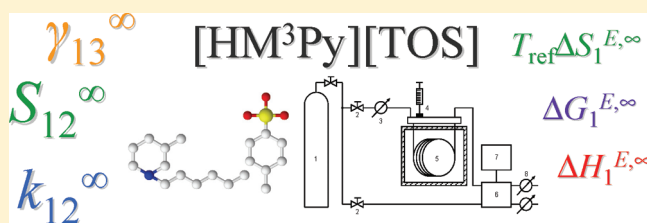


# Thermodynamics and Activity Coefficients at Infinite Dilution Measurements for Organic Solutes and Water in the Ionic Liquid *N*-Hexyl-3-methylpyridinium Tosylate

Urszula Domańska<sup>\*,†,‡</sup> and Marek Królikowski<sup>†</sup><sup>†</sup>Department of Physical Chemistry, Faculty of Chemistry, Warsaw University of Technology, Noakowskiego 3, 00-664 Warsaw, Poland<sup>‡</sup>Thermodynamic Research Unit, School of Chemical Engineering, University of KwaZulu—Natal, Howard College Campus, King George V Avenue, Durban 4001, South Africa

**ABSTRACT:** The activity coefficients at infinite dilution,  $\gamma_{13}^{\infty}$ , for 44 solutes, including alkanes, cycloalkanes, alkenes, alkynes, aromatic hydrocarbons, alcohols, water, thiophene, tetrahydrofuran, ethers, and ketones in the ionic liquid (IL) *N*-hexyl-3-methylpyridinium tosylate (*p*-toluenesulfonate), [HM<sup>3</sup>Py][TOS], were determined by gas–liquid chromatography at temperatures from 338.15 to 368.15 K. The densities of [HM<sup>3</sup>Py][TOS] as a function of temperature have been measured at temperatures higher than the melting temperature and were extrapolated to  $T = 298.15$  K. The gas–liquid partition coefficients,  $K_L$ , were calculated for all solutes. The partial molar excess Gibbs energies  $\Delta G_1^{E,\infty}$ , enthalpies  $\Delta H_1^{E,\infty}$ , and entropies  $\Delta S_1^{E,\infty}$  at infinite dilution were calculated from the experimental  $\gamma_{13}^{\infty}$  values obtained over the temperature range. The selectivities for different separation problems including *n*-heptane/benzene, cyclohexane/benzene, and *n*-heptane/thiophene were calculated from  $\gamma_{13}^{\infty}$  and compared to literature values for tosylate-based ILs, or hexyl-substituted cations of ILs, or pyridinium-based IL, or *N*-methyl-2-pyrrolidinone (NMP), and sulfolane.



## INTRODUCTION

Research of ionic liquids (ILs) is one of the most rapidly growing fields in the past 15 years. Due to their unique tunable physicochemical properties, ILs are creating the possibility of large-scale industrial applications. ILs are capable of dissolving a diverse range of inorganic, organic, and biomaterials. The solute–solvent interactions in solution is controlled by the nature and interplay of the cation and anion pair comprising the IL. These complex and dynamic interactions are the consequence of various energetic and geometric factors leading to uniquely organized, hydrogen-bonded, and self-segregated solvent nanostructures. For extraction processes, the essential solvent properties including selectivity and capacity can be directly calculated for different separation problems from the activity coefficients at infinite dilution,  $\gamma_{13}^{\infty}$ .<sup>1</sup> Recently, a careful analysis of published data of  $\gamma_{13}^{\infty}$  and obtained selectivities for the separation of the aliphatic hydrocarbons from aromatic hydrocarbons was presented for more than 70 ILs.<sup>2</sup>

This work is a continuation of our measurements of  $\gamma_{13}^{\infty}$  for tosylate-based ionic liquids (ILs).<sup>3,4</sup> Because of the aromatic anion of tosylate-based ILs, we expected that aliphatic hydrocarbons will be weakly soluble in tosylate-based ILs, whereas aromatic compounds will be very soluble.<sup>5–11</sup> The results of the solubility measurements in binary systems confirmed our expectations.<sup>5–11</sup> It was shown by us that benzene and *n*-alkylbenzenes have a high solubility in the ILs tetra-*n*-butylphosphonium tosylate, [B<sub>4</sub>P][TOS],<sup>6</sup> or in triisobutyl(methyl)phosphonium tosylate, [B<sub>3</sub>MP][TOS],<sup>7</sup> or in 1-butyl-3-methylimidazolium

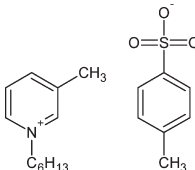
tosylate, [BMIM][TOS],<sup>8</sup> or in *N*-butyl-4-methylpyridinium tosylate (*p*-toluenesulfonate), [BM<sup>4</sup>Py][TOS],<sup>9</sup> or in *N*-butyl-3-methylpyridinium tosylate (*p*-toluenesulfonate), [BM<sup>3</sup>Py][TOS].<sup>10</sup> From the solid–liquid equilibria (SLE) of tosylate-based ILs as [BM<sup>4</sup>Py][TOS] or [BM<sup>3</sup>Py][TOS] or *N*-hexyl-3-methylpyridinium tosylate [HM<sup>3</sup>Py][TOS] or 1,4-dimethylpyridinium tosylate [M<sup>1,4</sup>Py][TOS] or 2,4,6-collidine tosylate [M<sup>2,4,6</sup>Py][TOS] in thiophene at ambient pressure, it was shown that these ILs can be used for the extraction of sulfur compounds from alkanes.<sup>11</sup> For example, the [BMIM][TOS] reveals simple eutectic mixtures with complete miscibility in the liquid phase in the binary systems containing water, or an alcohol and the eutectic systems with mutual immiscibility in the liquid phase with an upper critical solution temperature (UCST) in mixtures {[BMIM][TOS] + *n*-hexane or benzene or alkylbenzene or thiophene}.<sup>8</sup>

However, careful examination of the activity coefficients at infinite dilution of tosylate-based ILs have shown that the selectivities  $S_{ij}^{\infty}$  ( $S_{ij}^{\infty} = S_{i3}^{\infty}/\gamma_{j3}^{\infty}$ ) and capacities  $k_2^{\infty}$  ( $k_j^{\infty} = 1/\gamma_{j3}^{\infty}$ ) at infinite dilution for different solvents in ILs based on imidazolium or pyridinium or phosphonium cations with the tosylate anion have moderate values in the separation of aromatics or thiophene from aliphatics. It was shown that the pyridinium cation in the [BM<sup>4</sup>Py][TOS]<sup>9</sup> reveals much lower selectivities for separating aromatics from aliphatics than does [EMIM][TOS] (values extrapolated to the infinite dilution).<sup>12</sup>

Received: March 28, 2011

Published: May 18, 2011

Table 1. Investigated Ionic Liquid: Chemical Structure, Name, and Abbreviation

structure	name, abbreviation
	<i>N</i> -Hexyl-3-methylpyridinium tosylate, [HM <sup>3</sup> Py][TOS]

In the literature, there are numerous studies on tosylate-based ILs.<sup>13–18</sup> High-pressure study of the pure imidazolium tosylate IL<sup>13</sup> or the high-pressure solubility of carbon dioxide, CO<sub>2</sub>, was measured in the triisobutyl(methyl)phosphonium tosylate, P<sub>i</sub>(444)<sub>1</sub>TOS.<sup>14</sup> The solubility of adamantane and the  $\gamma_{13}^{\infty}$  in P<sub>i</sub>(444)<sub>1</sub>TOS was measured by the same group.<sup>15</sup> The 1-ethyl-3-methylimidazolium tosylate IL has shown moderate selectivity in the separation of *n*-hexane and aromatic compounds; the best about 5739 in ternary system IL + *n*-hexane + *rac*-1-phenylethyl propionate.<sup>16</sup> The liquid–liquid phase equilibria, LLE, of new tosylated hyperbranched polyglycerols were presented recently.<sup>17</sup> The ratio of total ion-pair binding energy to its dispersion component was well correlated with the melting temperature of tosylate-based IL and was close to bis(trifluoromethylsulfonyl) imide-based IL.<sup>18</sup>

We did not find any reports dealing with  $\gamma_{13}^{\infty}$  for *N*-hexyl-3-methylpyridinium tosylate (*p*-toluenesulfonate), [HM<sup>3</sup>Py][TOS]. Our research group has provided systematic measurements of  $\gamma_{13}^{\infty}$  for organic solutes and water in various ILs based on the pyridinium cation paired to different anions.<sup>3,19–22</sup> In two of these papers, we noted that ILs based on the thiocyanate anion<sup>20</sup> and trifluorotris(perfluoroethyl)phosphate-based (FAP) anion<sup>22</sup> present high extraction properties in many separation problems, including aromatic/aliphatics separation. However, careful analysis of our results indicates that the capacity of thiocyanate-based ILs is lower than those of FAP-based ILs and has room for improvement.<sup>20,22</sup>

In this work, we report the activity coefficients at infinite dilution,  $\gamma_{13}^{\infty}$ , for 44 solutes, including diverse *n*-alkanes, cycloalkanes, alkenes, alkynes, aromatic hydrocarbons, alcohols, water, thiophene, tetrahydrofuran (THF), ethers, acetone, and ketones, in the IL *N*-hexyl-3-methylpyridinium tosylate (*p*-toluenesulfonate), [HM<sup>3</sup>Py][TOS]. Values of  $\gamma_{13}^{\infty}$  were determined by gas–liquid chromatography at 10 K intervals from 338.15 to 368.15 K. This work also provides an opportunity to make comparisons with previously published results found in the literature and with other tosylate-based ILs.

## EXPERIMENTAL PROCEDURES

**Materials.** The ionic liquid [HM<sup>3</sup>Py][TOS] was synthesized in our laboratory. The synthesis and purity were described in our previous paper.<sup>23</sup> The sample was dried for several days at 300 K under reduced pressure to remove volatile impurities and trace water, resulting in a water content of <0.0003 mass fraction, as determined by Karl Fisher titration. The different solutes, purchased from Aldrich or Fluka, had purities better than 0.99 mass fraction and were used without further purification due to the fact that the GLC technique separates any impurities on

Table 2. Densities for Ionic Liquid [HM<sup>3</sup>Py][TOS] as a Function of Temperature

<i>T</i> /K	$\rho/\text{g}\cdot\text{cm}^{-3}$	<i>T</i> /K	$\rho/\text{g}\cdot\text{cm}^{-3}$
298.15 <sup>a</sup>	1.12701	353.15	1.09479
338.15	1.10386	358.15	1.09179
343.15	1.10078	363.15	1.08880
348.15	1.09778	368.15	1.08595

<sup>a</sup> Extrapolated value from equation:  $\rho = 6.10 \times 10^{-4}T + 1.3024$ .

the column. The structure of [HM<sup>3</sup>Py][TOS] is presented in Table 1.

**Density Measurements.** The density of [HM<sup>3</sup>Py][TOS] was measured using an Anton Paar GmbH 4500 vibrating-tube densimeter (Graz, Austria), thermostated at different temperatures. Two integrated Pt 100 platinum thermometers provided good precision of the internal control of temperature ( $\pm 0.01$  K), and the densimeter includes an automatic correction for the viscosity of the sample. The apparatus is precise to within  $1 \times 10^{-5} \text{ g cm}^{-3}$ , and the overall uncertainty of the measurements was estimated to be better than  $5 \times 10^{-5} \text{ g cm}^{-3}$ . Densimeter calibration was performed at atmospheric pressure using doubly distilled and degassed water, specially purified benzene (CHEMIPAN, Poland 0.999), and dried air. The densities of [HM<sup>3</sup>Py][TOS] over a temperature range (338.15–368.15) K are listed in Table 2.

**Apparatus and Experimental Procedure.** Experiments were performed using a PerkinElmer Clarus 500 gas chromatograph equipped with a thermal conductivity detector (TCD). The data were collected and processed using TotalChrom Workstation software. The column preparation and the packing method used in this work have been described in detail previously.<sup>2–4,19–22</sup> Glass columns of length 1 m and 4 mm internal diameter were used. Coating the solid support material with the IL was performed by dispersing a certain portion of Chromosorb in a methanol solution of the [HM<sup>3</sup>Py][TOS], followed by evaporation of the solvent using a rotary evaporator. The masses of the stationary phase and of the solid support were weighed with a precision  $\pm 0.0001$  g, achieving an uncertainty in [HM<sup>3</sup>Py][TOS] loading on the column on the order of  $2 \times 10^{-4}$  mmol. The solvent column packing varied from 45.05 (6.4715 mmol) to 38.59 (4.8729 mmol) mass percent of [HM<sup>3</sup>Py][TOS]. The large packing prevent possible residual adsorption of solute onto the column packing. Care was taken to ensure that the methanol was completely removed from the IL-coated solid support prior to column fabrication. Prior to each experiment, the column was conditioned by blowing hot carrier gas through it at a high flow rate ( $\sim 2.0 \text{ cm}^3 \cdot \text{s}^{-1}$ ) at 370 K for about 8 h. The pressure drop ( $P_i - P_o$ ) was varied between 60 and 80 kPa depending on flow rate of the carrier gas. The inlet pressure,  $P_i$ , was measured by a pressure gauge installed on the gas chromatograph with an

**Table 3.** Average Experimental Activity Coefficients at Infinite Dilution  $\gamma_{13}^{\infty}$  for the Organic Solutes and Water in Ionic Liquid [HM<sup>3</sup>Py][TOS] at Different Temperatures

solute	T/K			
	338.15	348.15	358.15	368.15
<i>n</i> -pentane	12.7	11.3	10.2	9.07
<i>n</i> -hexane	14.1	13.3	12.6	11.9
3-methylpentane	14.8	13.4	12.0	10.8
2,2-dimethylbutane	20.3	17.5	15.1	12.9
<i>n</i> -heptane	17.9	16.4	15.2	14.0
<i>n</i> -octane	22.3	20.9	19.7	18.3
2,2,4-trimethylpentane	25.7	23.1	21.0	18.8
<i>n</i> -nonane	28.0	26.6	24.9	23.5
<i>n</i> -decane	37.2	34.8	32.5	30.2
cyclopentane	5.46	5.05	4.71	4.38
cyclohexane	7.30	6.73	6.19	5.75
methylcyclohexane	9.50	8.83	8.28	7.72
cycloheptane	7.80	7.32	6.92	6.46
cyclooctane	8.99	8.47	8.02	7.54
1-pentene	7.08	6.54	6.02	5.58
1-hexene	8.44	7.89	7.42	6.99
cyclohexene	4.11	3.93	3.77	3.59
1-heptene	10.5	10.0	9.54	9.09
1-octene	13.5	12.8	12.3	11.6
1-decene	22.4	21.3	20.4	19.3
1-hexyne	2.24	2.27	2.33	2.35
1-heptyne	2.78	2.83	2.87	2.90
1-octyne	3.60	3.65	3.68	3.72
benzene	1.22	1.22	1.23	1.24
toluene	1.74	1.75	1.76	1.77
ethylbenzene	2.44	2.44	2.44	2.44
<i>o</i> -xylene	2.20	2.20	2.21	2.21
<i>m</i> -xylene	2.53	2.54	2.54	2.54
<i>p</i> -xylene	2.52	2.53	2.53	2.53
methanol	0.195	0.198	0.200	0.202
ethanol	0.291	0.292	0.294	0.295
1-propanol	0.329	0.33	0.333	0.335
water	0.220	0.228	0.236	0.244
thiophene	0.753	0.765	0.776	0.787
tetrahydrofuran	1.31	1.29	1.26	1.24
1,4-dioxane	1.16	1.14	1.15	1.15
methyl <i>tert</i> -butyl ether	4.84	4.57	4.34	4.09
methyl <i>tert</i> -pentyl ether	5.50	5.27	5.08	4.87
diethyl ether	4.00	3.83	3.67	3.51
di- <i>n</i> -propyl ether	7.46	7.09	6.78	6.54
di- <i>n</i> -butyl ether	12.7	11.9	11.4	10.8
acetone	1.21	1.19	1.18	1.16
2-pentanone	1.82	1.80	1.79	1.78
3-pentanone	1.81	1.80	1.79	1.78

uncertainty of  $\pm 0.1$  kPa and the outlet pressure,  $P_o$ , was measured using an Agilent precision gas flow meter having an uncertainty of  $\pm 0.07$  kPa.

The carrier gas was helium. The flow rate of carrier gas was determined using an Agilent precision gas flow meter which was placed at the outlet after the detector and had an uncertainty of

$\pm 0.1$  mL  $\cdot$  min<sup>-1</sup>. The flow rate was set for a series of runs and was allowed to stabilize for at least 15 min before any  $\gamma_{13}^{\infty}$  determinations were made. The flow rates were duly corrected for water vapor pressure. Solute injections ranged from 0.01 to 0.3  $\mu$ L and can be considered to be at “infinite dilution” on the column.

Temperature-dependent experiments were carried out in 10 K steps from 338.15 to 368.15 K. The temperature of the column was maintained constant to within  $\pm 0.02$  K. At a given temperature, each experiment was repeated two to three times to establish reproducibility. Retention times were generally reproducible to within  $10^{-3}$ – $10^{-2}$  min depending upon the temperature and the individual solute. At each temperature, values of the dead time,  $t_G$ , equivalent to the retention time of a completely nonretained component were also measured. While our GC was equipped with a TCD detector, air was used as a nonretainable component. The estimated overall error in  $\gamma_{13}^{\infty}$  was less than 3%, taking into account the possible errors in determining the column loading, the retention times, and solute vapor pressure. Our GLC technique was validated using the hexane in hexadecane system at 298.15 K and the results compared very favorably with the literature values.<sup>24</sup> The resulted activity coefficient values as a function of temperature are summarized in Table 3.

## THEORETICAL BASIS

The equations developed by Everett<sup>25</sup> and Cruickshank et al.<sup>26</sup> were used in this work to calculate  $\gamma_{13}^{\infty}$  for solutes in [HM<sup>3</sup>Py][TOS].

$$\ln \gamma_{13}^{\infty} = \ln \left( \frac{n_3 RT}{V_N P_1^*} \right) - \frac{P_1^* (B_{11} - V_1^*)}{RT} + \frac{P_o J_2^3 (2B_{12} - V_1^{\infty})}{RT} \quad (1)$$

In this expression,  $n_3$  is the number of moles of solvent on the column packing,  $R$  is the gas constant,  $T$  is the column temperature,  $V_N$  denotes the net retention volume of the solute,  $P_1^*$  is the saturated vapor pressure of the solute at temperature  $T$ ,  $B_{11}$  is the second virial coefficient of pure solute,  $V_1^*$  is the molar volume of the solute,  $P_o$  is the outlet pressure,  $P_o J_2^3$  is the mean column pressure,  $B_{12}$  (where the subscript “2” refers to the carrier gas, in this case helium) is the mixed second virial coefficient of the solute and carrier gas, and  $V_1^{\infty}$  is the partial molar volume of the solute at infinite dilution in the solvent. The thermophysical properties required in developing the activity coefficients at infinite dilution were calculated using equations and constants proposed in the literature.<sup>27</sup> The values of  $B_{12}$  were calculated using the Tsonopolous equation<sup>28</sup> using the parameters described as well.<sup>29</sup> The pressure correction term,  $J_2^3$ , is given by

$$J_2^3 = \frac{2}{3} \frac{(P_i/P_o)^3 - 1}{(P_i/P_o)^2 - 1} \quad (2)$$

The net retention volume of the solute,  $V_N$ , is given by

$$V_N = J_2^3 U_o (t_R - t_G) \quad (3)$$

where  $t_R$  and  $t_G$  are the retention times for the solute and an unretained gas, respectively, and  $U_o$  is the column outlet flow rate, corrected for the vapor pressure of water by

$$U_o = U \left( 1 - \frac{P_w}{P_o} \right) \frac{T}{T_i} \quad (4)$$

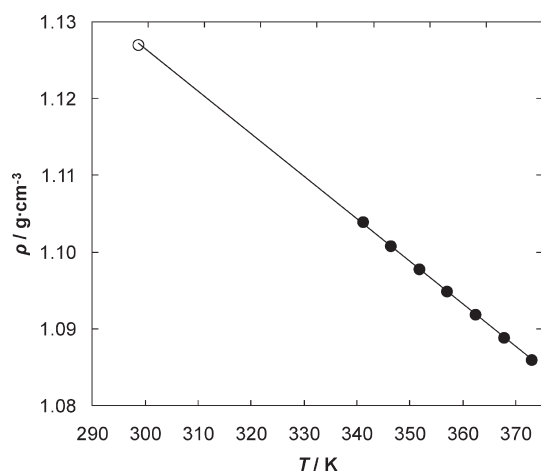


**Figure 1.** Plot of the density as a function temperature for [HM<sup>3</sup>Py][TOS]. Solid line represents the linear approximation.

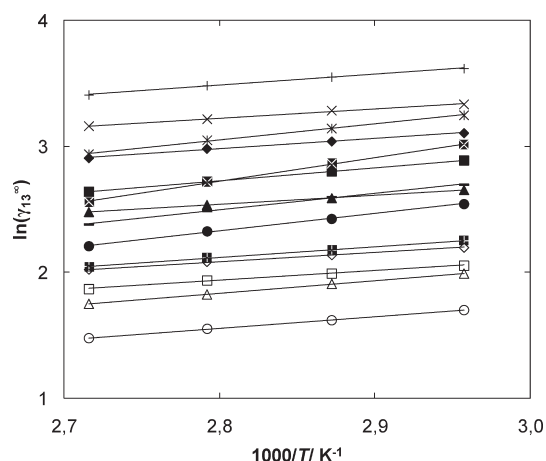


**Figure 2.** Plot of  $\ln(\gamma_{13}^{\infty})$  for ionic liquid [HM<sup>3</sup>Py][TOS] vs  $1/T$  for the solutes: (●) *n*-pentane; (▲) *n*-hexane; (—) 3-methylpentane; (white ×) 2,2-dimethylbutane; (■) *n*-heptane; (◆) *n*-octane; (\*) 2,2,4-trimethylpentane; (×) *n*-nonane; (+) *n*-decane; (○) cyclopentane; (Δ) cyclohexane; (white +) methylcyclohexane; (□) cycloheptane; and (◇) cyclooctane.

where  $T_f$  is the temperature at the column outlet,  $P_w$  is the vapor pressure of water at  $T_b$  and  $U$  is the flow rate measured with the flow meter.

While the activity coefficients at infinite dilution are determined as a function of temperature,  $\ln \gamma_{13}^{\infty}$  can be split to its respective enthalpic and entropic components

$$\ln \gamma_{13}^{\infty} = \frac{\Delta H_1^{E,\infty}}{RT} - \frac{\Delta S_1^{E,\infty}}{R} \quad (5)$$

Assuming that the temperature dependence follows a linear van't Hoff plot

$$\ln \gamma_{13}^{\infty} = a/T + b \quad (6)$$

the partial molar excess enthalpy,  $\Delta H_1^{E,\infty} = Ra$ , at infinite dilution can be obtained from the slope.

The gas–liquid partition coefficient  $K_L = (c_1^L/c_1^G)$  for a solute partitioning between a carrier gas and the [HM<sup>3</sup>Py][TOS] was

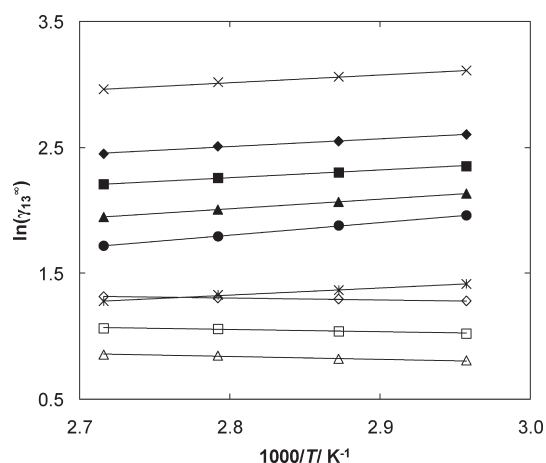


**Figure 3.** Plot of  $\ln(\gamma_{13}^{\infty})$  for ionic liquid [HM<sup>3</sup>Py][TOS] vs  $1/T$  for the solutes: (●) pent-1-ene; (▲) hex-1-ene; (\*) cyclohexene; (■) hept-1-ene; (◆) oct-1-ene; (Δ) hex-1-yne; (□) hept-1-yne; and (◇) oct-1-yne.

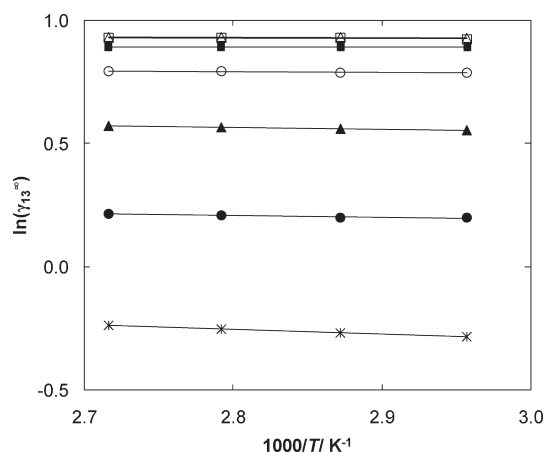


**Figure 4.** Plot of  $\ln(\gamma_{13}^{\infty})$  for ionic liquid [HM<sup>3</sup>Py][TOS] vs  $1/T$  for the solutes: (●) benzene; (▲) toluene; (■) ethylbenzene; (○) *o*-xylene; (Δ) *m*-xylene; (□) *p*-xylene; and (\*) thiophene.

calculated from the solute retention according to the following equation

$$\ln(K_L) = \ln\left(\frac{V_N \rho_3}{m_3}\right) - \frac{P_o J_2^3 (2B_{12} - V_1^{\infty})}{RT} \quad (7)$$

in which  $\rho_3$  is the density of the solvent ([HM<sup>3</sup>Py][TOS]).

## RESULTS AND DISCUSSION

The densities, presented in Table 2 and in Figure 1, decrease as usual with an increase of temperature. The density of [HM<sup>3</sup>Py][TOS] at  $T = 298.15$  K is  $1.12701 \text{ g} \cdot \text{cm}^{-3}$ .

The values of  $\gamma_{13}^{\infty}$ , listed in Table 3, show dependencies on temperature. Figures 2–6 present the natural logarithm of the activity coefficient for [HM<sup>3</sup>Py][TOS] as a function of the inverse absolute temperature for all investigated solutes. The influence of temperature follows the typical trend in ILs. With an increase in temperature, a decrease in  $\gamma_{13}^{\infty}$  is observed for most of the solutes including the *n*-alkanes, cycloalkanes, alkenes, acetone and other ketones, and ethers. For some solutes, however, the trend



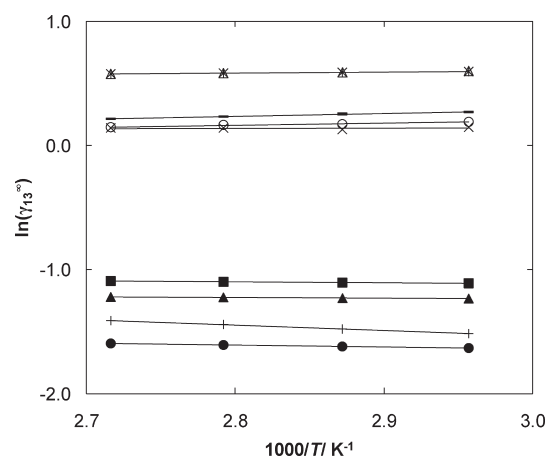


**Figure 5.** Plot of  $\ln(\gamma_{13}^{\infty})$  for ionic liquid  $[\text{HM}^3\text{Py}][\text{TOS}]$  vs  $1/T$  for the solutes: (●) methanol; (▲) ethanol; (■) 1-propanol; (X) 1,4-dioxane; (○) acetone; (△) pentan-2-one; (\*) pentan-3-one; (—) THF; and (+) water.

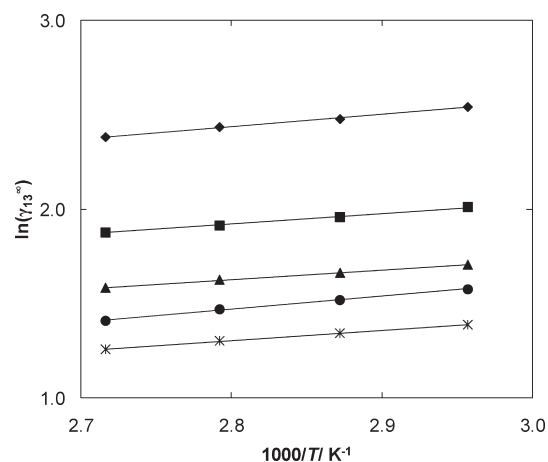


**Figure 6.** Plot of  $\ln(\gamma_{13}^{\infty})$  for ionic liquid  $[\text{HM}^3\text{Py}][\text{TOS}]$  vs  $1/T$  for the solutes: (●) MTBE; (▲) TAME; (\*) diethyl ether; (■) di-*n*-propyl ether; (◆) di-*n*-butyl ether.

with temperature is the opposite, especially for aromatic hydrocarbons, thiophene, alcohols, and water.

The values of  $\gamma_{13}^{\infty}$  for solute homologues increase with an increase in alkyl chain length. The highest  $\gamma_{13}^{\infty}$  values are observed for the *n*-alkanes, cycloalkanes, and alkenes. For example, for *n*-decane  $\gamma_{13}^{\infty} = 37.2$  at  $T = 338.15$  K. This behavior is typical of ILs, including the subset of those based on the pyridinium cation. High values of  $\gamma_{13}^{\infty}$  signify very weak interactions between solute and solvent. Cyclic alkanes show reduced values of  $\gamma_{13}^{\infty}$  in comparison to the corresponding linear *n*-alkanes. Similarly, the values of  $\gamma_{13}^{\infty}$  for alkynes are lower than those for alkenes for the same carbon number. This is related to the higher interaction strength between  $[\text{HM}^3\text{Py}][\text{TOS}]$  and the triple bond present in alkynes. Aromatic hydrocarbons reveal very strong interactions between the IL and the  $\pi$ -delocalized electrons in aromatic solutes and have even smaller  $\gamma_{13}^{\infty}$  values than alkynes. The smallest value between aromatic hydrocarbons is observed for thiophene,  $\gamma_{13}^{\infty} = 0.753$  at  $T = 338.15$  K. The small values of  $\gamma_{13}^{\infty}$  were found for alcohols, ethers, ketones, tetrahydrofuran (THF),

**Table 4.** Experimental Gas–Liquid Partition Coefficients  $K_L$  for the Organic Solutes and Water in Ionic Liquid  $[\text{HM}^3\text{Py}][\text{TOS}]$  at Different Temperatures

solute	T/K			
	338.15	348.15	358.15	368.15
<i>n</i> -pentane	3.10	2.76	2.49	2.30
<i>n</i> -hexane	7.32	5.93	4.86	4.06
3-methylpentane	5.89	5.00	4.37	3.90
2,2-dimethylbutane	2.94	2.70	2.51	2.39
<i>n</i> -heptane	15.1	11.9	9.51	7.8
<i>n</i> -octane	31.2	23	17.3	13.5
2,2,4-trimethylpentane	10.3	8.42	6.94	5.92
<i>n</i> -nonane	63.5	43.9	31.9	23.6
<i>n</i> -decane	122	82.2	57.1	41.0
cyclopentane	10.3	8.71	7.4	6.4
cyclohexane	20.4	16.5	13.7	11.4
methylcyclohexane	29.2	22.9	18.2	14.9
cycloheptane	65.5	49.4	37.9	30.1
cyclooctane	173	124	90.3	68.2
1-pentene	4.67	4.05	3.59	3.21
1-hexene	10.4	8.46	6.98	5.87
cyclohexene	38.7	30.1	23.9	19.4
1-heptene	21.7	16.7	13.1	10.5
1-octene	43.6	32	23.9	18.5
1-decene	168	113	77.7	55.4
1-hexyne	50.0	37.0	27.7	21.4
1-heptyne	103	73.0	52.9	39.3
1-octyne	203	137	95.7	68.4
benzene	120	88.9	67.0	51.5
toluene	230	163	118	87.5
ethylbenzene	400	273	191	137
<i>o</i> -xylene	598	402	277	196
<i>m</i> -xylene	432	293	204	146
<i>p</i> -xylene	418	284	198	142
methanol	457	319	227	166
ethanol	536	363	252	180
1-propanol	1071	695	465	321
water	1620	1041	690	469
thiophene	223	161	119	90.4
tetrahydrofuran	71.3	54.6	42.7	34.0
1,4-dioxane	267	193	139	104
methyl tert-butyl ether	14.1	11.5	9.52	8.12
methyl tert-pentyl ether	32.8	25.2	19.8	15.9
diethyl ether	9.08	7.49	6.3	5.39
di- <i>n</i> -propyl ether	27.6	21.1	16.5	13.1
di- <i>n</i> -butyl ether	103	72.4	51.5	38.4
acetone	57.3	44.3	34.7	27.8
2-pentanone	175	125	91.7	68.7
3-pentanone	173	124	91.1	68.3

and water ( $\gamma_{13}^{\infty} = 0.220$  at  $T = 338.15$  K). It is possible to assume the hydrogen bonding between these polar compounds and anion of the  $[\text{HM}^3\text{Py}][\text{TOS}]$ . Only the tertiary ethers show higher than linear ethers values of  $\gamma_{13}^{\infty}$ .

As is apparent from the entries in Table 4, the gas–liquid partition coefficients,  $K_L$ , for a solute decrease with an increase in

**Table 5.** Limiting Partial Molar Excess Gibbs Energies,  $\Delta G_1^{E,\infty}$ , Enthalpies,  $\Delta H_1^{E,\infty}$ , and Entropies,  $T_{\text{ref}}\Delta S_1^{E,\infty}$ , for the Organic Solutes and Water in Ionic Liquid  $[\text{HM}^3\text{Py}][\text{TOS}]$  at the Reference Temperature  $T_{\text{ref}} = 338.15 \text{ K}$

solute	$\Delta G_1^{E,\infty} / \text{kJ} \cdot \text{mol}^{-1}$	$\Delta H_1^{E,\infty} / \text{kJ} \cdot \text{mol}^{-1}$	$T_{\text{ref}}\Delta S_1^{E,\infty} / \text{kJ} \cdot \text{mol}^{-1}$
<i>n</i> -pentane	7.1	12	4.4
<i>n</i> -hexane	7.4	5.8	−1.6
3-methylpentane	7.6	11	3.3
2,2-dimethylbutane	8.5	16	7.1
<i>n</i> -heptane	8.1	8.4	0.3
<i>n</i> -octane	8.7	6.7	−2.0
2,2,4-	9.1	11	1.6
trimethylpentane			
<i>n</i> -nonane	9.4	6.1	−3.3
<i>n</i> -decane	10.2	7.2	−3.0
cyclopentane	4.8	7.6	2.8
cyclohexane	5.6	8.3	2.7
methylcyclohexane	6.3	7.1	0.8
cycloheptane	5.8	6.4	0.7
cyclooctane	6.2	6.0	−0.2
1-pentene	5.5	8.2	2.7
1-hexene	6.0	6.5	0.5
cyclohexene	4.0	4.6	0.7
1-heptene	6.6	5.0	−1.6
1-octene	7.3	5.1	−2.2
1-decene	8.7	5.1	−3.7
1-hexyne	2.3	−1.8	−4.0
1-heptyne	2.9	−1.5	−4.3
1-octyne	3.6	−1.1	−4.7
benzene	0.6	−0.58	−1.1
toluene	1.6	−0.59	−2.1
ethylbenzene	2.5	0.0	−2.5
<i>o</i> -xylene	2.2	−0.19	−2.4
<i>m</i> -xylene	2.6	−0.12	−2.7
<i>p</i> -xylene	2.6	−0.13	−2.7
methanol	−4.6	−1.2	3.4
ethanol	−3.5	−0.49	3.0
1-propanol	−3.1	−0.65	2.5
water	−4.3	−3.6	0.7
thiophene	−0.8	−1.5	−0.7
tetrahydrofuran	0.8	1.9	1.2
1,4-dioxane	0.4	0.19	−0.2
methyl <i>tert</i> -butyl ether	4.4	5.8	1.3
methyl <i>tert</i> -pentyl ether	4.8	4.2	−0.6
diethyl ether	3.9	4.5	0.6
di- <i>n</i> -propyl ether	5.6	4.6	−1.1
di- <i>n</i> -butyl ether	7.1	5.5	−1.7
acetone	0.5	1.4	0.9
2-pentanone	1.7	0.75	−0.9
3-pentanone	1.7	0.58	−1.1

temperature as for many ILs. Conversely, the highest values are observed for ketones, alcohols, water, and ethers. For solute homologues, the values of  $K_L$  increase with an increase in an alkyl

**Table 6.** Selectivities,  $S_{12}^\infty$ , and Capacities,  $k_{12}^\infty$ , at Infinite Dilution for Several Ionic Liquids, NMP, and Sulfolane for Different Separation Problems at  $T = 338.15 \text{ K}$

ionic liquid	$S_{12}^\infty$			$k_{12}^\infty$
	<i>n</i> -heptane/ benzene	cyclohexane/ benzene	<i>n</i> -heptane/ thiophene	benzene
$[\text{HM}^3\text{Py}][\text{TOS}]$	14.7	5.98	23.8	0.82
$[\text{BM}^4\text{Py}][\text{TOS}]^a$	12.8	4.42	—	0.25
$[\text{BMIM}][\text{TOS}]^b$	24.5	8.32	43.3	0.51
$[\text{HMIM}][\text{NTf}_2]^c$	12.8	6.43	—	1.42
$[\text{HMIM}][\text{BF}_4]^d$	24.4	9.68	—	1.06
$[\text{HMIM}][\text{PF}_6]^e$	17.7	7.50	—	0.93
$[\text{HMIM}][\text{SCN}]^f$	31.5	10.4	47.2	0.49
$[\text{HMIM}][\text{CF}_3\text{SO}_3]^g$	16.8	6.79	—	0.64
$[\text{EPy}][\text{NTf}_2]^h$	28.0	10.1	—	0.70
$[\text{BM}^4\text{Py}][\text{BF}_4]^i$	45.6	14.6	—	0.61
$[\text{BM}^4\text{Py}][\text{NTf}_2]^j$	20.8	9.22	23.6	1.33
$[\text{BM}^4\text{Py}][\text{SCN}]^k$	57.3	15.1	95.6	0.58
$[\text{BM}^3\text{Py}][\text{CF}_3\text{SO}_3]^l$	22.8	8.74	30.9	0.79
$[\text{3OH-C}_3\text{Py}][\text{FAP}]^l$	40.8	16.2	42.2	1.05
NMP <sup>m</sup>	—	5.73	—	0.94
sulfolane <sup>n</sup>	19.6	6.40	—	0.43

<sup>a</sup> Reference 3. <sup>b</sup> Reference 30. <sup>c</sup> Reference 31. <sup>d</sup> Reference 32. <sup>e</sup> Reference 33. <sup>f</sup> Reference 34. <sup>g</sup> Reference 35. <sup>h</sup> Reference 36. <sup>i</sup> Reference 37. <sup>j</sup> Reference 19. <sup>k</sup> Reference 20. <sup>l</sup> Reference 21. <sup>m</sup> Reference 22. <sup>n</sup> Reference 38. <sup>o</sup> Reference 39.

chain length or in the number of carbons in the ring sported by the solute. Low values of  $K_L$  signify low interactions between solute and solvent. It can be explained by the van der Waals interaction between *n*-alkane chain and the *n*-hexyl substituent of the pyridinium cation. Cyclic alkanes show higher values of  $K_L$  in comparison to the corresponding linear *n*-alkanes. Similarly, the values of  $K_L$  for alkynes are higher than those for *n*-alkenes for the same carbon number. This interaction is usually related to the  $\pi$ – $\pi$  interaction between  $[\text{HM}^3\text{Py}][\text{TOS}]$  and the triple bond present in alkynes. Aromatic hydrocarbons have higher  $K_L$  values than alkynes, which indicates the higher interaction between the IL, composed of the pyridinium cation and tosylate anion, and the  $\pi$ -delocalized electrons in aromatic solutes. The highest values of  $K_L$  were found for water (1620 at  $T = 338.15 \text{ K}$ ) and 1-propanol (1071 at  $T = 338.15 \text{ K}$ ). Overall, when the IL–solute interaction decreases, the value of  $K_L$  increases.

A comparison of these data with 1-ethyl-3-methylimidazolium tetracyanoborate,  $[\text{EMIM}][\text{TCB}]$ , results determined earlier by our group<sup>29</sup> evidence the similar trends of changes of  $K_L$ . For  $[\text{EMIM}][\text{TCB}]$ , the values of  $K_L$  for the *n*-alkanes were the lowest and the value for water was the highest and in the same order of magnitude.

$\Delta G_1^{E,\infty}$  is a basic thermodynamic function, calculated from our GLC data, which again informs us about fundamental interactions between solute and solvent. The  $\Delta G_1^{E,\infty}$  values are positive for most of the solutes. The negative values are only for alcohols, water, and thiophene. The entropy,  $T_{\text{ref}}\Delta S_1^{E,\infty}$ , is small and negative for most of the solutes studied.

The partial molar excess enthalpies at infinite dilution,  $\Delta H_1^{E,\infty}$ , determined from the Gibbs–Helmholtz equation, alongside other thermodynamic functions, are listed in Table 5. The general changes in  $\Delta H_1^{E,\infty}$  are as usual for the *n*-alkane,

cycloalkane, and alkene groups. The calculated values are positive (4.6–12) for these solutes. The values of  $\Delta H_1^{E,\infty}$  for alkynes, benzene, toluene, xylenes, alcohols, water, thiophene, and THF are all small and negative. The  $\Delta H_1^{E,\infty}$  values for benzene, toluene, and the xylenes are seen to range from  $-0.12$  to  $-0.59$  kJ mol $^{-1}$ . The error in  $\Delta H_1^{E,\infty}$  is the same as for the linear regression of the natural logarithm of the activity coefficient as a function of the inverse absolute temperature.

The main parameters in designing an effective extraction process are the selectivity,  $S_{12}^\infty$ , and the capacity,  $k_2^\infty$ , of entrainers (in this case, [HM<sup>3</sup>Py][TOS]) which can be calculated directly from experimental  $\gamma_{13}^\infty$  values.<sup>1</sup>

Table 6 shows selectivities at infinite dilution for ILs based on different ions containing the tosylate anion and/or the imidazolium, or pyridinium cation with hexyl and butyl substituents for *n*-heptane/benzene, cyclohexane/benzene, and *n*-heptane/thiophene separations.<sup>19–22,30–39</sup>

For *n*-heptane/benzene, at  $T = 338.15$  K, the selectivity for [HM<sup>3</sup>Py][TOS] (14.7) is higher than for [BM<sup>4</sup>Py][TOS] (12.8);<sup>3</sup> the best between tosylate-based ILs is [BMIM][TOS] (24.5).<sup>30</sup> Several ILs containing the pyridinium-based cation have much better selectivity than [HM<sup>3</sup>Py][TOS], as, for example, [BM<sup>4</sup>Py][SCN] (57.3)<sup>20</sup> or [BM<sup>4</sup>Py][BF<sub>4</sub>] (45.6).<sup>37</sup>

For *n*-heptane/thiophene, at  $T = 338.15$  K, the selectivity for [HM<sup>3</sup>Py][TOS] is higher (23.8) than those for *n*-heptane/benzene; however, [BM<sup>4</sup>Py][SCN]<sup>20</sup> has much higher selectivity in this separation problem (95.6).<sup>20</sup>

The selectivity and capacity for [HM<sup>3</sup>Py][TOS] and the organic solvents as NMP and sulfolane<sup>38,39</sup> are comparable for different separation problems. Although in most cases the high values of selectivity of entrainers indicate low capacity, for [HM<sup>3</sup>Py][TOS] both selectivity and capacity show average values.

## CONCLUDING REMARKS

Activity coefficients at infinite dilution for 44 solutes in the IL [HM<sup>3</sup>Py][TOS] were measured by gas–liquid chromatography at the temperatures from 338.15 to 368.15 K and compared to data for other tosylate-based ILs and data from other laboratories for imidazolium-based and pyridinium-based ILs. The thermodynamic functions at infinite dilution and the gas–liquid partition coefficients for the same solutes were developed in [HM<sup>3</sup>Py][TOS]. The ability of different ILs as solvents for the separation of aromatic hydrocarbons or sulfur compounds from aliphatic hydrocarbons was demonstrated. The activity coefficients at infinite dilution values are the first approach for designing the selectivity and capacity of any extraction process.

## AUTHOR INFORMATION

### Corresponding Author

\*E-mail: ula@ch.pw.edu.pl. Fax: +48 22 6282741. Phone: +48 22 6213115.

## ACKNOWLEDGMENT

This work has been supported by the European Union in the framework of European Social Fund through the Warsaw University of Technology Development Programme.

## REFERENCES

- (1) Kato, R.; Gmehling, J. *J. Chem. Thermodyn.* **2005**, *37*, 603–619.
- (2) Marciniak, A. *Fluid Phase Equilib.* **2010**, *294*, 213–233.
- (3) Letcher, T. M.; Ramjugernath, D.; Królikowski, M.; Laskowska, M.; Naidoo, P.; Domańska, U. *Fluid Phase Equilib.* **2009**, *276*, 31–36.
- (4) Domańska, U.; Paduszyński, K. *J. Chem. Thermodyn.* **2010**, *42*, 707–711.
- (5) Domańska, U.; Casás, L. *J. Phys. Chem. B* **2007**, *111*, 4109–4115.
- (6) Domańska, U.; Paduszyński, K. *J. Phys. Chem. B* **2008**, *112*, 11054–11059.
- (7) Domańska, U.; Paduszyński, K. *Fluid Phase Equilib.* **2009**, *278*, 90–96.
- (8) Domańska, U.; Królikowski, M. *J. Chem. Thermodyn.* **2010**, *42*, 355–362.
- (9) Domańska, U.; Królikowski, M.; Pobudkowska, A.; Letcher, T. M. *J. Chem. Eng. Data* **2009**, *54*, 1435–1441.
- (10) Letcher, T. M.; Ramjugernath, D.; Tumba, K.; Królikowski, M.; Domańska, U. *Fluid Phase Equilib.* **2010**, *294*, 89–97.
- (11) Domańska, U.; Królikowski, M.; Slesińska, K. *J. Chem. Thermodyn.* **2009**, *41*, 1303–1311.
- (12) Mutelet, F.; Joubert, J.-N. *J. Chromatogr. A* **2006**, *1102*, 256–267.
- (13) Aparicio, S.; Aldade, R.; García, B.; Lad, J. M. *J. Phys. Chem. B* **2009**, *113*, 5593–5606.
- (14) Ventura, S. P. M.; Pauly, J.; Daridon, J. L.; Lopes da Silva, J. A.; Marrucho, I. A.; Dias, A. M. A.; Coutinho, J. A. P. *J. Chem. Thermodyn.* **2008**, *40*, 1187–1192.
- (15) Oliveira, F. S.; Freire, M. G.; Pratas, M. J.; Pauly, J.; Daridon, J. L.; Marrucho, I. A.; Coutinho, J. A. P. *J. Chem. Eng. Data* **2010**, *55*, 662–665.
- (16) Hernández-Fernández, F. J.; De los Ríos, A. P.; Gómez, D.; Rubio, M.; Tomás-Alonso, F.; Villora, G. *Fluid Phase Equilib.* **2008**, *263*, 190–198.
- (17) Tamaki, M.; Taguchi, T.; Kitayo, Y.; Takanashi, K.; Sakai, R.; Kakuchi, T.; Satoh, T. *J. Polym. Sci., Part A, Polym. Chem.* **2009**, *47*, 7032–7042.
- (18) Bernard, U. L.; Izgorodina, E. I.; MacFarlane, D. R. *J. Phys. Chem. C* **2010**, *114*, 20472–20478.
- (19) Domańska, U.; Marciniak, A. *J. Chem. Thermodyn.* **2009**, *41*, 1350–1355.
- (20) Domańska, U.; Królikowska, M. *J. Phys. Chem. B* **2010**, *114*, 8460–8466.
- (21) Marciniak, A.; Wlazło, M. *J. Chem. Eng. Data* **2010**, *55*, 3208–3211.
- (22) Marciniak, A.; Wlazło, M. *J. Phys. Chem. B* **2010**, *114*, 6990–6994.
- (23) Domańska, U.; Królikowski, M. *J. Chem. Thermodyn.* **2011**, accepted.
- (24) Tiegs, D.; Gmehling, J.; Medina, A.; Soares, M.; Bastos, J.; Alessi, P.; Kikic, I. *Activity Coefficients at Infinite Dilution, Chemistry Data Series*; Dechema: Frankfurt, 1986; Vol. IX, Part 1, p 586.
- (25) Everett, D. H. *Trans. Faraday Soc.* **1965**, *61*, 1637–1639.
- (26) Cruickshank, A. J. B.; Gainey, B. W.; Hicks, C. P.; Letcher, T. M.; Moody, R. W.; Young, C. L. *Trans. Faraday Soc.* **1969**, *65*, 1014–1031.
- (27) Design Institute for Physical Properties, sponsored by AIChE (2005; 2008; 2009; 2010). DIPPR Project 801, Full Version. Design Institute for Physical Property Research/AIChE. Online version available at: [http://knovel.com/web/portal/browse/display?\\_EXT\\_KNOVEL\\_DISPLAY\\_bookid=1187&VerticalID=0](http://knovel.com/web/portal/browse/display?_EXT_KNOVEL_DISPLAY_bookid=1187&VerticalID=0).
- (28) Poling, B. E.; Prausnitz, J. M. *Properties of Gases and Liquids*; McGraw-Hill Publishing: New York, 2001. Available from: <http://lib.mylibrary.com?ID=91317>.
- (29) Domańska, U.; Królikowska, M.; Acree, J. W. E.; Baker, G. A. *J. Chem. Thermodyn.* **2011**, *43*, 1050–1057.
- (30) Domańska, U.; Królikowski, M. *J. Chem. Eng. Data* **2010**, *55*, 4817–4822.
- (31) Letcher, T. M.; Marciniak, A.; Marciniak, M.; Domańska, U. *J. Chem. Thermodyn.* **2005**, *37*, 1327–1331.
- (32) Letcher, T. M.; Soko, B.; Reddy, P.; Deenadayalu, N. *J. Chem. Eng. Data* **2003**, *48*, 1587–1590.
- (33) Letcher, T. M.; Soko, B.; Ramjugernath, D.; Deenadayalu, N.; Nevines, A.; Naicker, P. K. *J. Chem. Eng. Data* **2003**, *48*, 708–711.
- (34) Domańska, U.; Marciniak, A.; Królikowska, M.; Arasimowicz, M. *J. Chem. Eng. Data* **2010**, *55*, 2532–2536.

- (35) Yang, X.-J.; Wu, J.-S.; Ge, M.-L.; Wang, L.-S.; Li, M.-Y. *J. Chem. Eng. Data* **2008**, 53, 1220–1222.
- (36) Kato, R.; Gmehling, J. *Fluid Phase Equilib.* **2004**, 226, 37–44.
- (37) Heintz, A.; Kulikov, D. V.; Verevkin, S. P. *J. Chem. Eng. Data* **2001**, 46, 1526–1529.
- (38) Krummen, M.; Gruber, D.; Gmehling, J. *Ind. Eng. Chem. Res.* **2000**, 39, 2114–2123.
- (39) Möllmann, C.; Gmehling, J. *J. Chem. Eng. Data* **1997**, 42, 35–40.